

# Magnetic properties of $AlB_2$ -type holmium silicides and germanides

G. Eguchi<sup>1</sup>, R. Matsumoto<sup>1</sup>, K. Terashima<sup>1</sup>, and Y. Takano<sup>1,2</sup>

<sup>1</sup>National Institute for Materials Science, 1-2-1 Sengen, Tsukuba, Ibaraki 305-0047,  
Japan

<sup>2</sup>University of Tsukuba, 1-1-1 Tennodai, Tsukuba, Ibaraki 305-8577, Japan

Keywords: Magnetism, Heavy rare earths, Hydrogen liquefaction

Email: eguchi.gaku@nims.go.jp

(Date: July 26, 2024)

## Abstract

Discovery of the large magnetocaloric effect in  $HoB_2$  has highlighted the practical advantage of heavy rare-earth ions. Other holmium compounds are of interest, and we here report the synthesis and the magnetic properties of  $HoSi_{1.67}$  and  $HoGe_{1.67}$  which form the same  $AlB_2$ -type structure but with vacancies. They are found to show the antiferromagnetic order with the Néel temperature 17.6(2) K for  $HoSi_{1.67}$  and 9.9(2) K for  $HoGe_{1.67}$ , and the magnetic entropy changes at the temperature are 0.05(1) J/cm<sup>3</sup>K for  $HoSi_{1.67}$  and 0.08(1) J/cm<sup>3</sup>K for  $HoGe_{1.67}$ . Magnetic orders were suppressed by replacing vacancies with nickel, resulting in an increase of magnetic entropy changes. Distance between the in-plane  $Ho^{3+}$  ions appears to be an important parameter leading to the transition between the antiferromagnetic ( $HoSi_{1.67}$ ) and the ferromagnetic ( $HoB_2$ ) order. The finding may aid the exploration of other heavy rare-earth compounds for similar applications.

## Introduction

Efficient refrigeration is one of the keys for reducing energy consumption and magnetocooling has the potential to make a significant impact on a global scale. Magnetic materials are used as coolants, and those with large magnetic moments are advantageous to increase the cooling capacity. For this purpose heavy rare-earths are particularly suitable as they are known to have the large local moments.

Hydrogen liquefaction is one of the applications [1, 2]. Recently, large magnetocaloric effect was found in the  $\text{HoB}_2$  near the boiling point of hydrogen [3]. It was proposed with the help of machine learning, and the finding highlights surprisingly rich functionalities that are still hidden in a simple rare-earth compound. Apparently the local moment on the  $\text{Ho}^{3+}$  ion, which is known to have the large value by a factor of 10.5 compared to the Bohr magneton ( $\mu_B$ ) [4], harbor the changes. Such large local moments are common to holmium compounds, and therefore, we reviewed the magnetic properties of binary  $\text{HoX}_2$ . One of the major categories is the Laves phase ( $X = \text{Al, Mn, Fe, Co, Ni, Ru, Rh, Re, Os, Ir, Pt}$ ) and they are known to show the ferromagnetic order [5-9]. Others ( $X = \text{H, C, Si, Cu, Zn, Ga, Ge, Ag, Au}$ ) take various crystal structures and they are known to show the antiferromagnetic order [10-18]. The above situation highlights peculiarity of the ferromagnetic order in the  $\text{HoB}_2$ . It forms so-called  $\text{AlB}_2$ -type structure, and one of the antiferromagnets  $\text{HoGa}_2$  forms the same structure. According to a database [19] there are two other compounds in the same form:  $\text{HoSi}_{1.7}$  and  $\text{HoGe}_{1.5}$  [20, 21], but their magnetic properties are not known. Figure 1 shows the lattice parameter, the magnetic order, and the magnetic entropy changes ( $-\Delta S$ ) reported so far [22, 23]. In terms of distance or concentration of  $\text{Ho}^{3+}$  ions the  $\text{HoSi}_{1.7}$  and  $\text{HoGe}_{1.5}$  lie in the intermediate range. They form the layered  $\text{Ho}^{3+}$  triangular lattice, which raises the question

of what magnetic properties they actually have. Likewise their potentially large  $-\Delta S$  associated with the geometrical frustration [24, 25].

We report the synthesis and the magnetic properties of  $\text{AlB}_2$ -type holmium silicides and germanides. Polycrystals were prepared by arc melting, and samples close to the single phase were obtained with the nominal compositions  $\text{HoSi}_{1.67}$  and  $\text{HoGe}_{1.67}$ . In contrast, melting with the composition  $\text{HoSi}_{2.00}$  resulted in a dimorph of tetragonal  $\text{ThSi}_2$ -type and orthorhombic  $\text{GdSi}_{1.4}$ -type structures. They all showed a decrease of the magnetization below a critical temperature, and the  $-\Delta S$  remained similar in amplitude to those of  $\text{HoGa}_2$  [23]. Vacancies at the Si or Ge sites can accommodate other elements [26] and we attempted to replace vacancies with nickel in order to control the magnetic properties. Nearly single-phase  $\text{HoGe}_{1.50}\text{Ni}_{0.50}$  was obtained and its properties were also investigated.

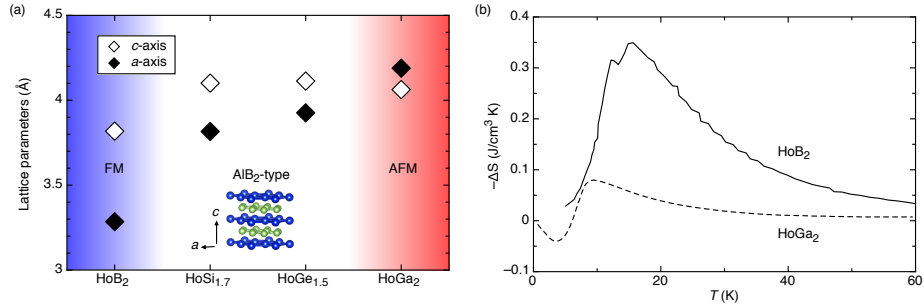


Figure 1: **The  $\text{AlB}_2$ -type binary holmium compounds found in the literature.** (a) Lattice parameter and magnetic order.  $\text{HoB}_2$  is known to show the ferromagnetic order (FM) and  $\text{HoGa}_2$  the antiferromagnetic order (AFM). Inset is a schematic of the  $\text{AlB}_2$ -type structure [27]. (b) Magnetic entropy changes from 5 T to 0 T in the  $\text{HoB}_2$  and in the  $\text{HoGa}_2$  [22, 23].

## Materials and methods

The Ho ingot, Si ingot, Ge powder, and Ni wire were purchased from a commercial vendor and they were reported to be 99.9 wt%, 99.999 wt%, 99.99 wt%,

99 wt% pure, respectively. Surface of the Ho ingots were sanded out and the oxide layer was removed, then they were cut into pieces. The pieces were roughly 100-300 mg in weight, and the amount of other materials was calculated according to the weight. The Si ingot was smashed and the Ni wire was cut. The Ge powder was formed into pellets after weighting. The above processes were carried out in the air. The samples were prepared by arc melting under an Ar atmosphere. The mixtures were turned over and melted several times to ensure homogeneity.

According to Pukas *et al.* [26] the AlB<sub>2</sub>-type silicides and germanides are stabilized with defects on the Si or Ge sites. A systematic investigation was required to obtain the target crystal structure, and we prepared samples with different compositions HoSi<sub>2.00</sub>, HoSi<sub>1.67</sub>, HoSi<sub>1.50</sub>, HoGe<sub>2.00</sub>, HoGe<sub>1.67</sub>, and HoGe<sub>1.50</sub>. The compositions are used as labels in this report. Powder x-ray diffraction was performed with a commercial diffractometer (Rigaku, MiniFlex600) with Cu-K $\alpha$  radiation ( $\lambda=1.5406 \text{ \AA}$ ) and the obtained patterns were analyzed using Rietan package [28]. We focused on the identification of crystal phases and lattice parameters. The lattice parameters were stable within the 3 significant figures and they are used to estimate the volume of the samples from the weight. Both the preparation of powder specimens and the measurements were carried out in the air at room temperature. We in addition prepared several pieces with the same recipe and one of the pieces was used for magnetization measurement without shaping. Its shape was nearly spherical, and thus, the demagnetization factor was assumed to be 1/3. All magnetization data reported in this paper are after the demagnetization correction. The dc magnetization was measured with a SQUID magnetometer (Quantum Design, MPMS-XL). We used a straw provided from the company and ensured that background signals were negligible.

## Results

Figure 2 shows the powder x-ray diffraction patterns and their fitting. Corresponding crystal images are also shown in the figure [27]. Various crystal phases have been reported in the holmium silicides and germanides [19], and the  $\text{HoSi}_{2.00}$  was found to be a dimorph of tetragonal  $\text{ThSi}_2$ -type structure and orthorhombic  $\text{GdSi}_{1.4}$ -type structure. Main phase of the  $\text{HoSi}_{1.50}$ ,  $\text{HoSi}_{1.67}$ , and  $\text{HoGe}_{1.67}$  was found to be the  $\text{AlB}_2$ -type structure. Additional peaks in the  $\text{HoSi}_{1.50}$  and the  $\text{HoSi}_{1.67}$  derive from foreign phases, which however could not be identified. Additional peaks in the germanide samples derive from the orthorhombic  $\text{DyGe}_2$ -type structure. The main phases and their lattice parameters are summarized in the Table 1.

Magnetic properties of the  $\text{HoSi}_{1.67}$ ,  $\text{HoGe}_{1.67}$ , and  $\text{HoSi}_{2.00}$  were investigated in detail. Figure 3(a) shows the magnetic field ( $\mu_0 H$ ) dependence of the magnetization ( $M$ ) for the  $\text{HoSi}_{1.67}$  at selected temperatures. The data at 6 K were collected with increasing the field after zero-field-cooling (ZFC), and afterwards with decreasing the field. Magnetic hysteresis was not detected as can be seen in the figure. Nonlinear field dependence was detected below 20 K. The  $M$  of the  $\text{HoGe}_{1.67}$  and the  $\text{HoSi}_{2.00}$  were collected using the same measurement sequence, and results were essentially similar (not shown). Figure 3(b) shows the temperature ( $T$ ) dependence of the magnetic susceptibility ( $\chi_{\text{dc}}$ ) at the weak field limit, obtained from the linear fitting of the  $M - H$  curve below 1 T (Fig. 3(a)), and the  $M/\mu_0 H$  obtained from the  $M - T$  curve under the field 10 mT. All  $\text{HoSi}_{1.67}$ ,  $\text{HoGe}_{1.67}$  and  $\text{HoSi}_{2.00}$  show a steep decrease below a critical temperature  $T^*$  at where  $\partial(M/H)/\partial T = 0$ , indicating a suppression of net magnetic moment. We in addition investigated the  $T$  dependence with ZFC and FC and confirmed the absence of hystereses in the whole measured temperature range (not shown). These results are consistent with the antiferromagnetic

order at the  $T^*$  with second-order phase transition.

Figure 3(c) shows the same data in the reciprocal susceptibility. The  $\mu_0 H/M$  above 95 K were well approximated by the linear temperature dependence and thus were fit with conventional Curie-Weiss model

$$\chi_{\text{dc}} = \frac{\mu_{\text{eff}}^2}{3k_{\text{B}}(T - T_{\text{CW}})} + \chi_0, \quad (1)$$

where  $\mu_{\text{eff}}$  is the effective magnetic moment,  $k_{\text{B}}$  is the Boltzmann constant,  $T_{\text{CW}}$  is the Curie-Weiss temperature, and  $\chi_0$  is the temperature-independent offset which is commonly referred to as the Pauli susceptibility. There are three open parameters  $\mu_{\text{eff}}$ ,  $T_{\text{CW}}$ , and  $\chi_0$ , and values obtained from the fitting are listed in the Table 1. The  $\mu_{\text{eff}}$  are fairly close to the  $10.5\mu_{\text{B}}$ , but small deviations are found. The  $\text{HoSi}_{1.67}$  have the largest  $\chi_0$  and  $T_{\text{CW}}$  values among the materials investigated in this study. It also showed the highest  $T^*$ . These results imply an enhancement of magnetic interaction in the  $\text{HoSi}_{1.67}$ .

Figure 4 shows the  $-\Delta S$  from 5T to 0T. They were calculated using the relation

$$-\Delta S = -\mu_0 \int_0^H \left( \frac{\partial M}{\partial T} \right)_H dH \quad (2)$$

and the  $M - T$  curves in the field 0.1 T, 0.5 T, 1 T, 2 T, 3 T, 4 T, and 5 T. The  $-\Delta S$  of  $\text{HoGa}_2$  are adopted from [23]. Their amplitudes remain moderate due to the change of sign in the  $\partial M/\partial T$  at the  $T^*$ , which are typical of antiferromagnetic phase transition. The  $-\Delta S$  at the  $T^*$  are listed in the Table 1.

We note that the results for the  $\text{HoSi}_{2.00}$  are overall similar to the previous studies on the  $\text{HoSi}_2$  and the  $\text{HoSi}_{1.9}$  [12, 29]. Small deviations in the obtained values are likely to be minor effects on the  $-\Delta S$ .

## Discussion

Sample	Main phase	$a$ (Å)	$c$ (Å)	Volume (Å <sup>3</sup> /f.u.)	$\mu_{\text{eff}}$ ( $\mu_{\text{B}}$ )	$\chi_0$ ( $10^{-2}\mu_{\text{B}}/\text{T f.u.}$ )	$T_{\text{CW}}$ (K)	$T^*$ (K)	$-\Delta S$ (5-0T) (J/cm <sup>3</sup> K)	Reference
HoB <sub>2</sub>	AlB <sub>2</sub> -type	3.2849	3.8183	35.68	-	-	25	-	0.35	[3, 22]
HoSi <sub>1.50</sub>	AlB <sub>2</sub> -type	3.81(1)	4.11(1)	51.7	-	-	-	-	-	This work
HoSi <sub>1.67</sub>	AlB <sub>2</sub> -type	3.82(1)	4.10(1)	51.9	10.30(4)	3.37(5)	6.5(8)	17.6(2)	0.05(1)	This work
HoSi <sub>2.00</sub>	ThSi <sub>2</sub> -type/	3.97(1)	13.31(1)	52.6	10.36(1)	-0.47(1)	1.0(1)	13.7(2)	0.06(1)	This work
HoGe <sub>1.67</sub>	AlB <sub>2</sub> -type	3.91(1)	4.12(1)	54.4	10.80(1)	0.17(1)	1.0(2)	9.9(2)	0.08(1)	This work
HoGe <sub>2.00</sub>	ThSi <sub>2</sub> -type	4.05(1)	13.67(1)	56.1	-	-	-	-	-	This work
HoGa <sub>2</sub>	AlB <sub>2</sub> -type	4.20	4.04	61.74	10.10(4)	-	-13.1(1)	8.0(1)	0.06	[15, 23]

Table 1: **Properties obtained from this study.** The  $a$ ,  $c$ , and volume are from the powder x-ray diffraction, and the  $\mu_{\text{eff}}$ ,  $\chi_0$ ,  $T_{\text{CW}}$ ,  $T^*$ , and  $-\Delta S$  are from the dc magnetization. The values for HoB<sub>2</sub> and HoGa<sub>2</sub> were taken from the literature for comparison.

Various crystal phases have been reported in the rare-earth silicides and germanides, and they involve natural defects at the Si or Ge sites [26]. We focused on the AlB<sub>2</sub>-type structure and the large local moment on the Ho<sup>3+</sup> ion, and investigated their magnetic properties. They are found to show the antiferromagnetic order, and thus, the present study has revealed that only HoB<sub>2</sub> shows the ferromagnetic order in the AlB<sub>2</sub>-type binary holmium compounds. The  $T^*$  which corresponds to the Néel temperature, the  $T_{\text{CW}}$ , and the Curie temperature ( $T_{\text{C}}$ ) are shown in the Fig. 5.  $T_{\text{CW}}$  represents the strength of the molecular field at high temperature and positive (negative) values are interpreted as ferromagnetic (antiferromagnetic) exchange interaction between the local moments. Reciprocal of the lattice parameter  $a$  is in addition shown in the figure; The  $a$  corresponds to the minimum distance between the Ho<sup>3+</sup> ions in the triangular lattice. Interestingly, the  $T_{\text{CW}}$  and the  $a$  have similar trends. This implies that the distance between the in-plane Ho<sup>3+</sup> ions is an important parameter for the magnetic exchange interaction. The  $T_{\text{CW}}$  were positive for both HoSi<sub>1.67</sub> and HoGe<sub>1.67</sub>, but their actual orders were antiferromagnetic. The difference indicates a temperature variation of dominant magnetic interaction.

Previous studies have pointed the prevalence of Ruderman-Kittel-Kasuya-Yoshida (RKKY) interaction in both HoB<sub>2</sub> and HoGa<sub>2</sub> [15, 22]. It implies the presence of complex magnetic interaction between the local and the itinerant

moments, and the same applies to the  $\text{HoSi}_{1.67}$  and the  $\text{HoGe}_{1.67}$ . Further decrease of the  $\text{Ho}^{3+}$  distance is most likely favorable for strengthening the ferromagnetic interaction, and thus, the decrease is also likely advantageous to increase the  $\partial M/\partial T$  (Eqn. 2) and the  $-\Delta S$ . We point out that the RKKY interaction is often considered to be prevalent in other magnetocaloric materials [30, 31]. As the distance between the ions are readily available from crystal structure analysis, detailed investigation of them may be useful in the search for other materials.

RKKY interaction is the exchange interaction between the local moments mediated by the itinerant spins, and accordingly, it is expected to be sensitive to the spin degree of freedom of the conducting carriers. We considered controlling magnetic properties in this direction. Our results of the sample synthesis appear to support the criterion suggested by Pukas *et al.* [26], and the vacancies at the Si or Ge sites can accommodate other elements. The valence electron in the Si or Ge is expected to be conducting, therefore, we have attempted to add polarized itinerant spins by replacing the vacancies with nickel [32, 33]. Figure 6 show the results; A dimorph of  $\text{ThSi}_2$ -type and  $\text{AlB}_2$ -type structures in the nominal composition  $\text{HoSi}_{1.67}\text{Ni}_{0.33}$ , and a nearly single phase of  $\text{AlB}_2$ -type structure in the  $\text{HoGe}_{1.50}\text{Ni}_{0.50}$ , are obtained. They did not show magnetic orders down to 5.5 K and there were increases in the  $-\Delta S$  compared to those of  $\text{HoGe}_{1.67}$ . These results support the idea of controlling the local moments using the vacancies, and also underpin the prevalence of RKKY interaction. Properties obtained from this study are listed in the Table 2.

Finally, let us not omit mentioning the magnetic structure in the ordered states. So far, an in-plane antiferromagnetic order in  $\text{HoGa}_2$  and an out-of-plane ferromagnetic order in  $\text{HoB}_2$  have been reported [15, 22]. Further insights of actual magnetic structures shall be investigated by neutron diffraction.

Sample	Main phase	$a$ (Å)	$c$ (Å)	Volume (Å <sup>3</sup> /f.u.)	$\mu_{\text{eff}}$ ( $\mu_{\text{B}}$ )	$\chi_0$ ( $10^{-2}\mu_{\text{B}}/\text{T f.u.}$ )	$T_{\text{CW}}$ (K)	Reference
HoSi <sub>1.67</sub> Ni <sub>0.33</sub>	AlB <sub>2</sub> -type	3.93(1)	4.02(1)	53.8	-	-	-	This work
HoSi <sub>1.67</sub> Ni <sub>0.33</sub>	ThSi <sub>2</sub> -type	3.98(1)	13.59(1)	53.7	-	-	-	This work
HoGe <sub>1.50</sub> Ni <sub>0.50</sub>	AlB <sub>2</sub> -type	4.08(1)	3.97(1)	57.1	10.74(1)	-0.12(1)	4.7(2)	This work

Table 2: **Properties obtained from this study.** The  $a$ ,  $c$ , and Volume are from the powder x-ray diffraction, and the  $\mu_{\text{eff}}$ ,  $\chi_0$ , and  $T_{\text{CW}}$  are from the dc magnetization.

## Conclusion

In summary, we investigated magnetic properties of the AlB<sub>2</sub>-type binary holmium silicides and germanides. They are found to show the antiferromagnetic order and the magnetic entropy changes were similar to those of HoGa<sub>2</sub>. The magnetic order was suppressed by substituting nickel for vacancies, and there were increases in the magnetic entropy changes. A correspondence is found between the Curie-Weiss temperature and the in-plane Ho<sup>3+</sup> distance. RKKY interaction is suggested as the prevailing interaction and a small Ho<sup>3+</sup> distance is likely favorable to strengthen the ferromagnetic interaction and to increase magnetic entropy changes.

## Funding sources

Authors acknowledge the financial support from the JST-Mirai Program (Grant No. JPMJMI18A3) and JSPS KAKENHI (Grant Nos. 20K05070, 23K04572, 19H02177).

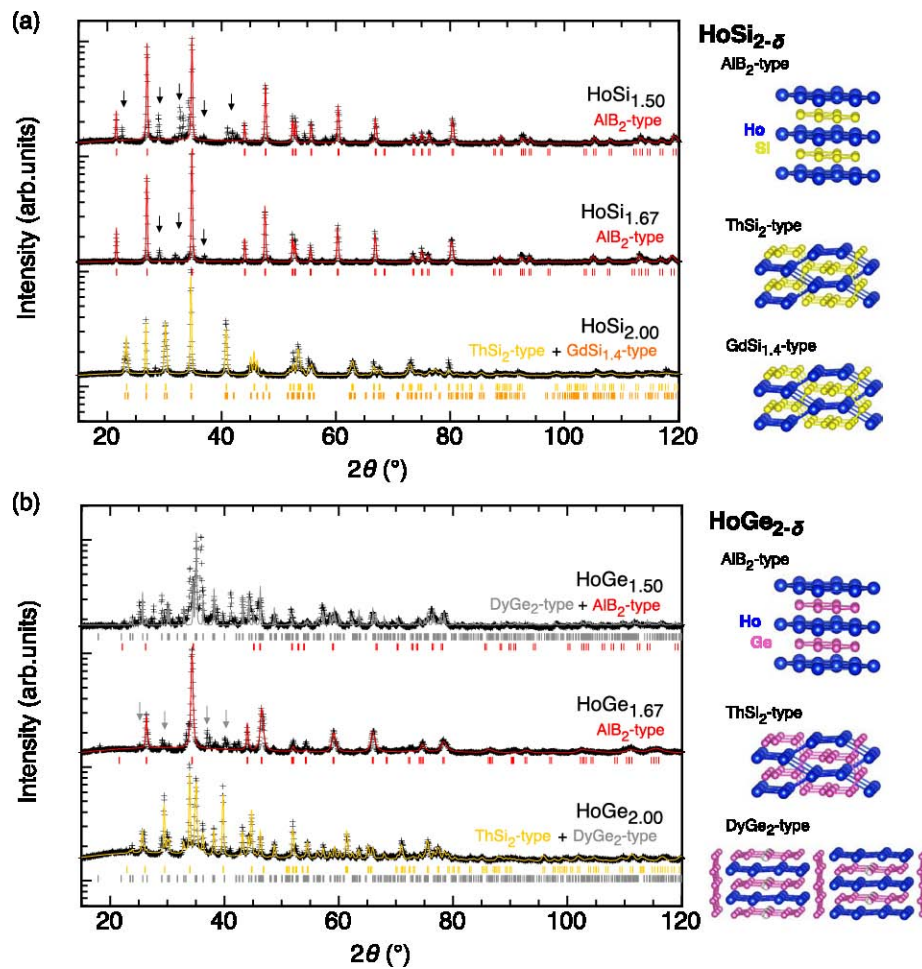


Figure 2: Powder x-ray diffraction patterns and their fitting. (a)  $\text{HoSi}_{2-\delta}$  and (b)  $\text{HoGe}_{2-\delta}$ . Corresponding crystal images are shown in the right panel. Additional peaks pointed by arrows are from unknown phases.

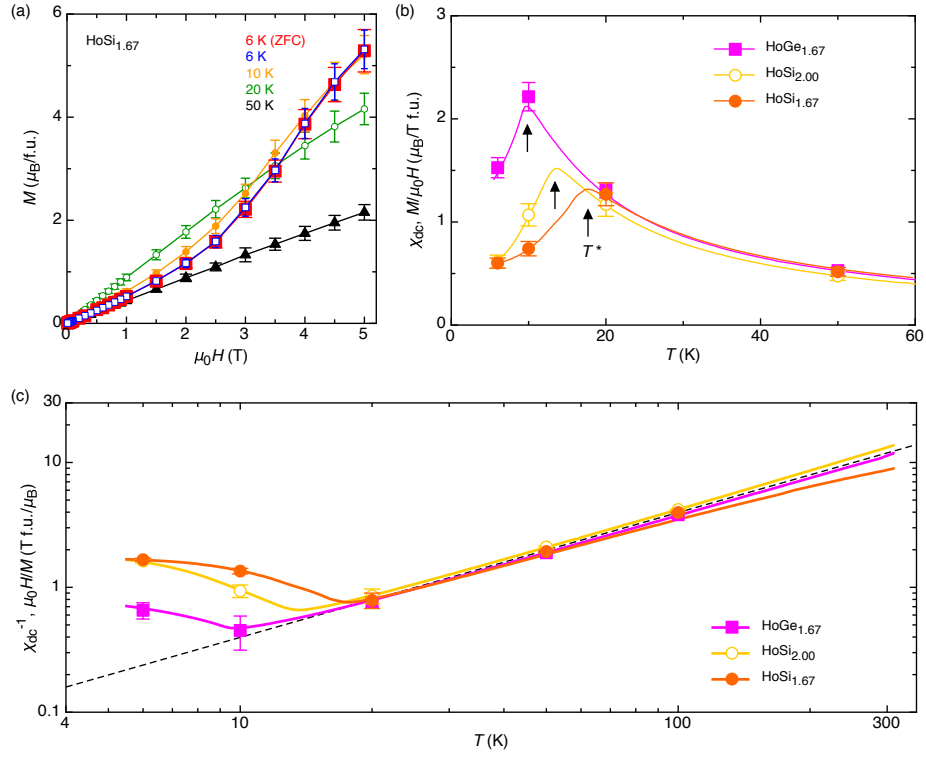


Figure 3: **Magnetization and magnetic susceptibility.** (a)  $M - H$  curve of the  $\text{HoSi}_{1.67}$  at selected temperatures. (b) Temperature dependence of the magnetic susceptibility. Arrows indicate the critical temperature  $T^*$ . (c) Temperature dependence of the reciprocal susceptibility. The broken line is a simulated curve of the Curie-Weiss model (Eqn.1) with  $\mu_{\text{eff}} = 10.5 \mu_B$ ,  $T_{\text{CW}} = 0$ , and  $\chi_0 = 0$ .

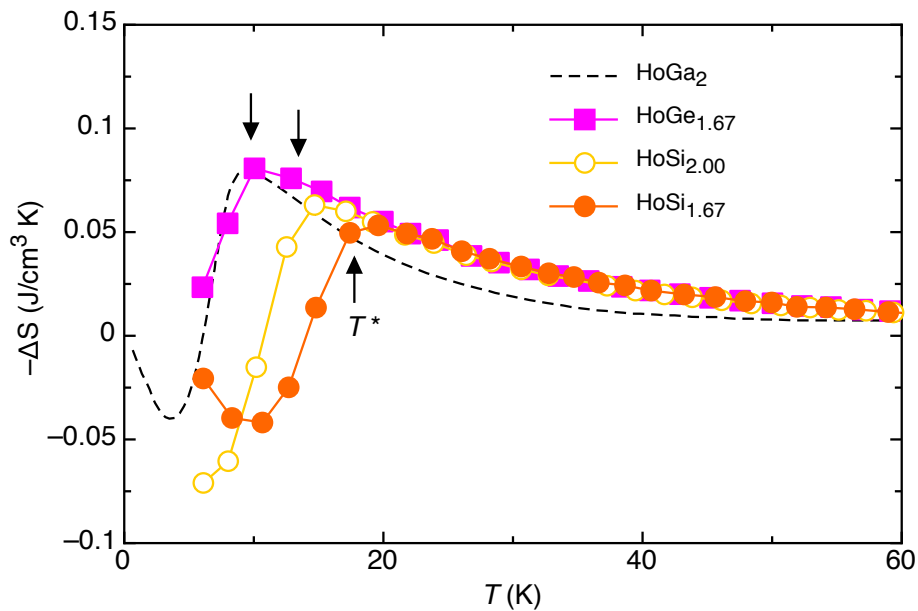


Figure 4: **Magnetic entropy changes from 5 T to 0 T.** Arrows indicate the  $T^*$ . The broken line is the same curve shown in the Fig. 1(b).

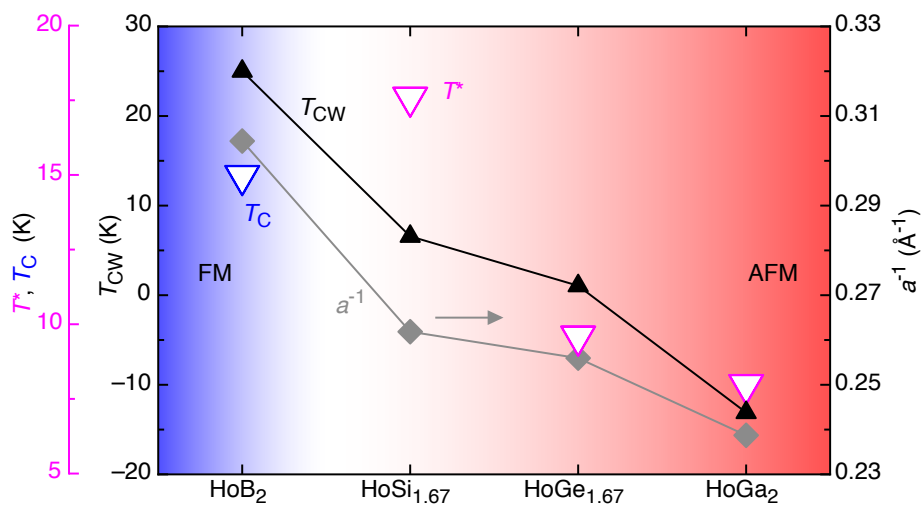


Figure 5: **Magnetic transition temperature and Curie-Weiss temperature.** FM stands for ferromagnetic order and AFM for antiferromagnetic order. Reciprocal of the lattice parameter  $a$  is also shown.

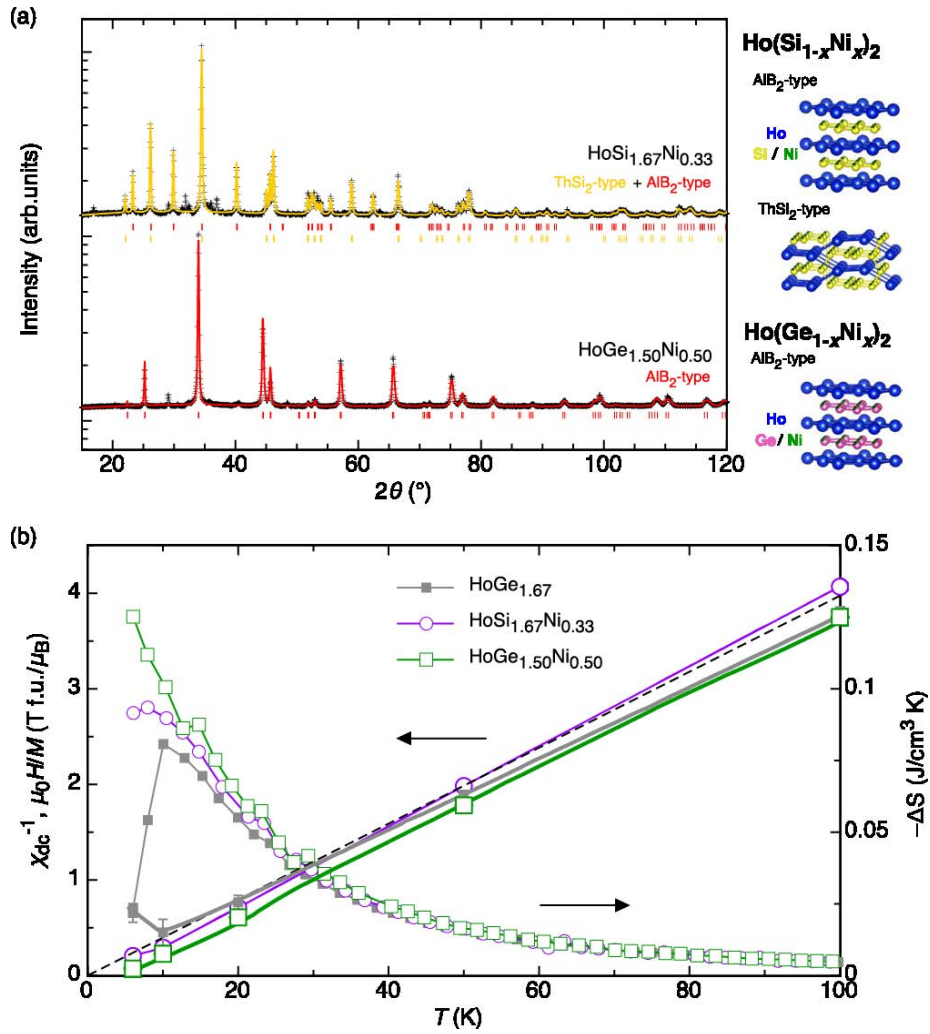


Figure 6: **Substitution of nickel for vacancies at the Si or Ge sites.** (a) Powder x-ray diffraction patterns and their fitting for  $\text{HoSi}_{1.67}\text{Ni}_{0.33}$  and  $\text{HoGe}_{1.50}\text{Ni}_{0.50}$ . Corresponding crystal images are shown in the right panel. (b) Temperature dependence of the reciprocal susceptibility and the magnetic entropy changes from 5 T to 0 T. The data of the  $\text{HoGe}_{1.67}$  are the same as those shown the Fig. 3(c) and Fig. 4. The broken line is the same curve shown in the Fig. 3(c).

## References

- [1] Saif ZS. Al Ghafri, Stephanie Munro, Umberto Cardella, Thomas Funke, William Notardonato, J. P. Martin Trusler, Jacob Leachman, Roland Span, Shoji Kamiya, Garth Pearce, Adam Swanger, Elma Dorador Rodriguez, Paul Bajada, Fuyu Jiao, Kun Peng, Arman Siahvashi, Michael L. Johns, and Eric F. May. Hydrogen liquefaction: a review of the fundamental physics, engineering practice and future opportunities. *Energy Environ. Sci.*, 15:2690–2731, 2022.
- [2] Numazawa T., Kamiya K., Utaki T., and Matsumoto K. Magnetic refrigerator for hydrogen liquefaction. *Progress in Superconductivity and Cryogenics*, 15(2):1–8, 06 2013.
- [3] Pedro Baptista de Castro, Kensei Terashima, Takafumi D. Yamamoto, Zhufeng Hou, Suguru Iwasaki, Ryo Matsumoto, Shintaro Adachi, Yoshito Saito, Peng Song, Hiroyuki Takeya, and Yoshihiko Takano. Machine-learning-guided discovery of the gigantic magnetocaloric effect in hcb2 near the hydrogen liquefaction temperature. *NPG Asia Materials*, 12(1):35, 2020.
- [4] Helena Kurzen, Laura Bovigny, Claudio Bulloni, and Claude Daul. Electronic structure and magnetic properties of lanthanide 3+ cations. *Chemical Physics Letters*, 574:129–132, 2013.
- [5] T. Hashimoto, T. Kuzuhara, M. Sahashi, K. Inomata, A. Tomokiyo, and H. Yayama. New application of complex magnetic materials to the magnetic refrigerant in an Ericsson magnetic refrigerator. *Journal of Applied Physics*, 62(9):3873–3878, 11 1987.

- [6] E. Talik, M. Kulpa, A Winiarski, T. Mydlarz, and M. Neumann. Electronic structure and magnetic properties of homn2 single crystals. *Journal of Alloys and Compounds*, 316(1):51–57, 2001.
- [7] T. Nakamichi Laves phase, magnetism. *Bulletin, The Japan Institute of Metals and Materials*, 7(2):63–72, 1968.
- [8] R. M. Bozorth, B. T. Matthias, H. Suhl, E. Corenzwit, and D. D. Davis. Magnetization of compounds of rare earths with platinum metals. *Phys. Rev.*, 115:1595–1596, Sep 1959.
- [9] M I Slanicka, K N R Taylor, and G J Primavesi. Moment variation in rare earth-transition metal c15 compounds of type afe2-aco2, aco2-ani2. *Journal of Physics F: Metal Physics*, 1(5):679, sep 1971.
- [10] J. N. Daou and P. Vajda. Role of hydrogen-sublattice ordering for magnetic and metal-semiconductor transitions in  $\beta$ -hoh<sub>2+x</sub>. *Phys. Rev. B*, 50:12635–12642, Nov 1994.
- [11] M. Atoji. Magnetic structures of tbc2 and hoc2. *Physics Letters*, 23(3):208–209, 1966.
- [12] Kazuko Sekizawa and Kō Yasukōchi. Antiferromagnetism of disilicides of heavy rare earth metals. *Journal of the Physical Society of Japan*, 21(2):274–278, 1966.
- [13] Yuzo Hashimoto, Hironobu Fujii, Hiroshi Fujiwara, and Tetsuhiko Okamoto. Magnetic properties of rare earth copper intermetallic compounds, rcu2. ii. light rare earth. *Journal of the Physical Society of Japan*, 47(1):73–76, 1979.
- [14] D. Debray and M. Sougi. Magnetic Structure of HoZn2. *The Journal of Chemical Physics*, 57(5):2156–2189, 09 1972.

- [15] T. H. Tsai and D. J. Sellmyer. Magnetic ordering and exchange interactions in the rare-earth gallium compounds  $rga_2$ . *Phys. Rev. B*, 20:4577–4583, Dec 1979.
- [16] Kazuko Sekizawa. Magnetic and crystallographic studies on rare earth germanides. *Journal of the Physical Society of Japan*, 21(6):1137–1142, 1966.
- [17] Masao Atoji. Magnetic Structure of HoAg<sub>2</sub>. *The Journal of Chemical Physics*, 51(9):3882–3885, 11 1969.
- [18] Masao Atoji. Magnetic Structure of HoAu<sub>2</sub>. *The Journal of Chemical Physics*, 57(6):2402–2406, 09 1972.
- [19] D. Zagorac, H. Müller, S. Ruehl, J. Zagorac, and S. Rehme. Recent developments in the Inorganic Crystal Structure Database: theoretical crystal structure data and related features. *Journal of Applied Crystallography*, 52(5):918–925, Oct 2019.
- [20] Li Jungin, Zhuang Yinghong, and Lin Weibo. Investigation of the ternary system ho - fe - si at 500 °c. *International Journal of Materials Research*, 84(11):773–775, 1993.
- [21] V. N. Jeremenko, Yi. M. Obushenko, and Yu. Yi. Buyanov. Phase diagram of holmium-germanium system. (7):69–71, 1980.
- [22] Noriki Terada, Kensei Terashima, Pedro Baptista de Castro, Claire V. Colin, Hiroaki Mamiya, Takafumi D. Yamamoto, Hiroyuki Takeya, Osamu Sakai, Yoshihiko Takano, and Hideaki Kitazawa. Relationship between magnetic ordering and gigantic magnetocaloric effect in hob<sub>2</sub> studied by neutron diffraction experiment. *Phys. Rev. B*, 102:094435, Sep 2020.

- [23] R D dos Reis, L M da Silva, A O dos Santos, A M N Medina, L P Cardoso, and F G Gandra. Study of the magnetocaloric properties of the antiferromagnetic compounds  $\text{R}_2\text{Ga}_2$  ( $\text{R} = \text{Ce, Pr, Nd, Dy, Ho}$  and  $\text{Er}$ ). *Journal of Physics: Condensed Matter*, 22(48):486002, nov 2010.
- [24] Yoshifumi Tokiwa, Sebastian Bachus, Kavita Kavita, Anton Jesche, Alexander A. Tsirlin, and Philipp Gegenwart. Frustrated magnet for adiabatic demagnetization cooling to milli-kelvin temperatures. *Communications Materials*, 2(1):42, 2021.
- [25] Christopher D O'Neill, Julian L Schmeh, Harry D J Keen, Luke Pritchard Cairns, Dmitry A Sokolov, Andreas Hermann, Didier Wermeille, Pascal Manuel, Frank Krüger, and Andrew D Huxley. Non-fermi liquid behavior below the néel temperature in the frustrated heavy fermion magnet  $\text{U}_2\text{Ga}_2$ . *Proceedings of the National Academy of Sciences of the United States of America*, 118(49):e2102687118, December 2021.
- [26] S. Pukas and R. Gladyshevskii. Structural defects of rare-earth disilicides and digermanides. *Chem. Met. Alloys*, pages 36–44, 2020.
- [27] Koichi Momma and Fujio Izumi. *VESTA3* for three-dimensional visualization of crystal, volumetric and morphology data. *Journal of Applied Crystallography*, 44(6):1272–1276, Dec 2011.
- [28] Fujio Izumi and T. Ikeda. A rietveld-analysis program rietan-98 and its applications to zeolites. In *European Powder Diffraction 6*, volume 321 of *Materials Science Forum*, pages 198–205. Trans Tech Publications Ltd, 1 2000.
- [29] J Pierre, E Siaud, and D Frachon. Magnetic properties of rare earth disilicides  $\text{R}_2\text{Si}_2$ . *Journal of the Less Common Metals*, 139(2):321–329, 1988.

- [30] Noriki Terada and Hiroaki Mamiya. High-efficiency magnetic refrigeration using holmium. *Nature Communications*, 12(1):1212, 2021.
- [31] P. M. Gehring, M. B. Salamon, A. del Moral, and J. I. Arnaudas. Magnetic static and scaling properties of the weak random-axis magnet  $(\text{d}_{xy}1-x)\text{al}_2$ . *Phys. Rev. B*, 41:9134–9147, May 1990.
- [32] J. Callaway and C. S. Wang. Self-consistent calculation of energy bands in ferromagnetic nickel. *Phys. Rev. B*, 7:1096–1103, Feb 1973.
- [33] J. F. Janak. Uniform susceptibilities of metallic elements. *Phys. Rev. B*, 16:255–262, Jul 1977.